

Compact Ultra-Wideband Antenna with Triple Band Notch Characteristics Using EBG Structures

Mahadu A. Trimukhe* and Balaji G. Hogade

Abstract—A compact ultra-wideband (UWB) antenna with triple band-notch characteristics is proposed. The proposed antenna employs fractal and two via edge located (TVEL) electromagnetic band gap (EBG) structures near the feed line to cause triple frequency band notch characteristics over WiMAX (3.3 to 4.0 GHz), WLAN (5.1 to 5.8 GHz), and satellite downlink communication (7.2 to 7.8 GHz) frequency bands. The proposed antenna is designed and fabricated on a $24 \times 24 \times 1.6 \text{ mm}^3$ FR4 substrate. It offers impedance bandwidth (VSWR < 2) from 2.9 to 11.2 GHz except over the notched bands. The antenna has nearly omnidirectional radiation patterns and steady gain over the desired UWB. The measured results agree with the simulated ones.

1. INTRODUCTION

Ultra-wideband systems have gained the attention from researches due to high data rate capacity, low power consumption, low cost, reduced interference, and precise localisation and positioning. UWB systems operate over 3.1–10.6 GHz frequency band, as assigned by the Federal Communications Commission (FCC) in the year 2002 [1].

UWB technology, however, interferes with adjacent narrow microwave frequency bands, viz. WiMAX (3.3–3.6 GHz), WLAN for IEEE 802.11a (5.15–5.35 GHz and 5.725–5.825 GHz), and ITU downlink satellite communication (7.25–7.75 GHz). Band-stop filters can be used to reduce interference from these bands, but these increase the cost and system size. Therefore, a compact UWB antenna with multi-band notch characteristics is in demand and of interest to current researchers.

Various techniques have been employed to realise UWB antennas with band-notch characteristics [2–16]. Slots of different shapes, such as U shape slot, U shape slot with parasitic strip, three C shape slot, and inverted U slots, have been introduced in the radiating patch and ground plane in [2–7]. The effective length of resonating slots of different shapes is about half a wavelength. Introducing a slot is a useful technique to achieve band-notch characteristic [2, 4]. Multiple slots can be designed to achieve multi-band notch characteristics [3, 5, 6]; however, multiple slots affect the gain, efficiency, and radiation pattern of an antenna. Another technique is the insertion of a resonator structure (such as split ring resonator and electric ring resonator) to obtain band-notch characteristics [8–10]. However, these techniques are difficult to design. Recently, EBG structures have been used in various antenna designs since they reduce surface waves, spurious response and improve the antenna efficiency [11]. EBG structures are used to design a compact UWB antenna with band notches in [12–17]. In [12], a single band notch circular shape UWB antenna is designed using four centre located via (CLV) EBG structures on a $39 \times 35 \text{ mm}^2$ substrate. Single CLV-EBG and edge located via (ELV) EBG are used [13], to obtain single band notch in an elliptic shape UWB antenna on $38 \times 40 \text{ mm}^2$ substrate. In [14], two spiral EBGs are used to obtain dual band notches. The antenna is designed on a Ro4350B substrate of $30 \times 35 \text{ mm}^2$ dimension. Four CLV EBG structures are used in [15], to achieve dual band notches in

Received 9 April 2019, Accepted 22 May 2019, Scheduled 5 June 2019

* Corresponding author: Mahadu Annarao Trimukhe (mahadu2005@gmail.com).

The authors are with the Department of Electronics and Telecommunication, Terna Engineering College, Navi-Mumbai, India.

a circular shape UWB antenna on a $42 \times 50 \text{ mm}^2$ substrate. A dual band notch elliptical shape UWB antenna ($38 \times 40 \text{ mm}^2$) which uses a single two via double slot (TVDS) EBG to obtain band notches over 4.38–4.70 GHz and 5.56–6.28 GHz has been reported [17]. The antenna structures in [12–16] have large dimensions and use multiple EBG structures to achieve dual band notch characteristics. In [17], dual band notches are achieved by using a single TVDS-EBG, but the antenna size is large.

In this paper, a novel and compact UWB antenna with triple band notch characteristics using two EBG structures is proposed. TVEL-EBG structure is used to achieve WiMAX and X band notch while a fractal EBG structure obtains WLAN band notch.

2. ANTENNA GEOMETRY AND DESIGN THEORY

2.1. UWB Antenna

The geometry of the proposed antenna with design parameters is depicted in Fig. 1. The antenna is designed using a 1.6 mm thick FR4 substrate having dielectric constant and loss tangent of 4.4 and 0.02, respectively.

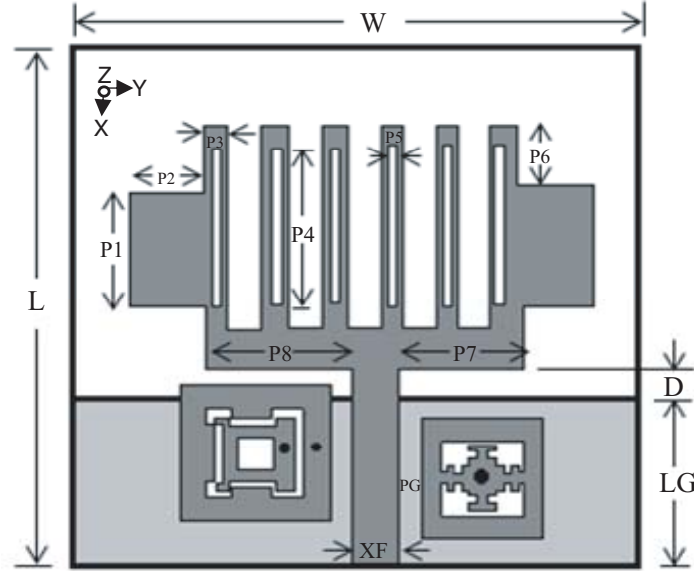


Figure 1. Geometrical structure of the proposed antenna.

Optimized parameters of the antenna are $L = 24 \text{ mm}$, $W = 24 \text{ mm}$, $P1 = 6 \text{ mm}$, $P2 = 2 \text{ mm}$, $P3 = 1.9 \text{ mm}$, $P4 = 6.6 \text{ mm}$, $P5 = 0.4 \text{ mm}$, $P6 = 1.9 \text{ mm}$, $P7 = 5.6 \text{ mm}$, $P8 = 6.2 \text{ mm}$, $D = 2.2 \text{ mm}$, $XF = 3 \text{ mm}$, $LG = 7.6 \text{ mm}$, $PG = 0.30 \text{ mm}$.

The structure is designed using multiple branches to resonate at different but close by frequencies which electromagnetically couple with each other to provide UWB. To reduce the size of the antenna slots are introduced in each branch since slots increase the effective current density and path length. Now triple band notch characteristics are achieved by introducing two EBG structures viz. TVEL-EBG and fractal EBG. The antenna is fed using a 50Ω microstrip line. Antenna structures are simulated and optimized using High-Frequency Structures Simulator (HFSS) software. The effective current path length $Le1$ corresponding to the central resonating frequency of the lowest band (f_{r1}) can be calculated using Eq. (1).

$$\begin{aligned} Le1 &= (D + 0.5XF + P8 + P6 + P2 + P1 + P2 + P6) \\ f_{r1} &= 7.2/Le1 \end{aligned} \quad (1)$$

The calculated value of $Le1$ for $f_{r1} = 3.1 \text{ GHz}$ is 23.7, while the simulated value is 23.2. The slight discrepancy is because Eq. (1) does not take into account the effect of thickness and permittivity of the

substrate.

The two EBG structures used near the feed line to achieve desired band notches are discussed in following subsection.

2.2. EBG Structure

EBG structures behave as a parallel LC circuit, and current flowing through via and ground plane results in an inductor L while the gap between the adjacent EBG units results in capacitance C [18]. The values of L in Henry and C in Farad are approximately given by [18].

$$L = \mu_0 h \tag{2}$$

where $\mu_0 =$ permeability of free space, $h =$ substrate height, and

$$C = \frac{\omega_1 \epsilon_0 (\epsilon_r + 1)}{\pi} \cos^{-1} \left\{ \frac{2\omega_1 + pg}{pg} \right\} \tag{3}$$

where w_1 is the width of the EBG metal patch; PG is the gap between two EBG cells; ϵ_0 and ϵ_r are the permittivity of air and relative permittivity of the substrate, respectively. Bandgap BW is approximately determined by [18].

$$BW = \frac{\Delta\omega}{\omega} \tag{4}$$

Geometry and equivalent L-C circuits of TVEL and Fractal EBG are shown in Fig. 2 and Fig. 3, respectively. In TVEL EBG, capacitance C_1 is predominantly due to outer slot. L_1 is due to the current flowing in via close to feed line and outer rectangular metallic ring. The nonuniform width of outer slot helps in achieving wideband notch. C_3 is due to inner slot and inductance L_3 due to current flowing in inner via and inner rectangular metallic strip. In fractal EBG, C_2 is due to slots and L_2 due to current flowing in the center located via and fractal metallic patch. Central band notch frequencies of TVLE and fractal EBG structures can be given as:

$$f_{ci} = \frac{1}{2\pi\sqrt{L_i C_i}} \tag{5}$$

Here $i = 1, 3$ is for TVLE and $i = 2$ for fractal EBG structures.

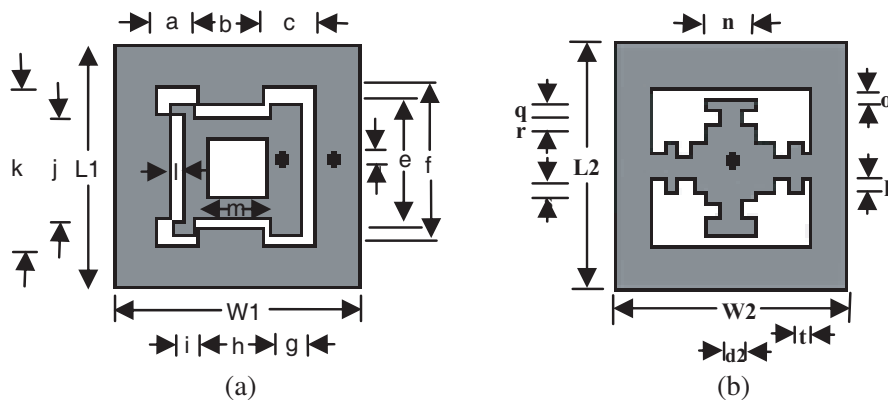


Figure 2. Geometries of the EBGs. (a) TVEL EBG. (b) Fractal EBG.

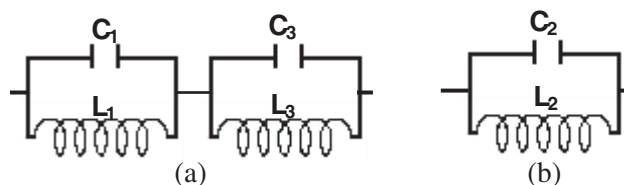


Figure 3. Equivalent circuits. (a) TVEL EBG. (b) Fractal EBG.

2.3. Evolution of Fractal EBG

A conventional square mushroom-type EBG has dimensions $< 0.1\lambda_0 \times 0.1\lambda_0$ where λ_0 is the free space wavelength corresponding to central band notch frequency [12, 13]. A fractal EBG with unit dimensions of $4.4 \text{ mm} \times 4.8 \text{ mm}$ is designed to reduce the dimension of conventional EBG. Fig. 4 shows the unit element of same dimensions of the fractal EBG and conventional mushroom-type EBG. The conventional EBG offers band notch characteristics from 5.6–6.2 GHz while fractal EBG structure rejects WLAN frequency band from 5.1 to 5.8 GHz. The dimension of fractal EBG is 11% less than that of conventional EBG. It also offers improved wideband notch characteristics compared to conventional EBG.

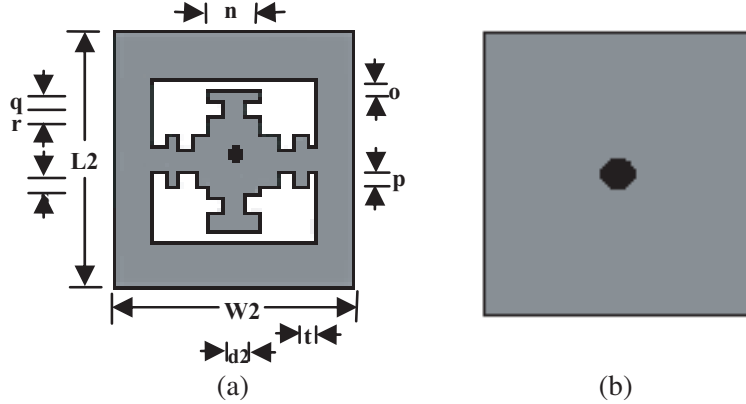


Figure 4. (a) Fractal EBG. (b) Conventional mushroom EBG.

The parameters for fractal EBG are: $W2 = 4.4 \text{ mm}$, $L2 = 4.8 \text{ mm}$, $n = 1 \text{ mm}$, $o = 0.2 \text{ mm}$, $p = 0.25 \text{ mm}$, $q = 0.3 \text{ mm}$, $r = 0.25 \text{ mm}$, $s = 0.25 \text{ mm}$, $t = 0.25 \text{ mm}$, $d2 = 0.94 \text{ mm}$.

Evolution of fractal EBG is shown in Fig. 5. As the metallic surface area decreases in fractal EBG, the magnitude of effective surface current density increases, and inductance increases. Beside this, the impedance of fractal EBG becomes more resistive than the conventional EBG. The gap between the metallic strips of fractal EBG results in capacitance; therefore, capacitance increases in a fractal EBG. The capacitive effect dominates over the inductive effect; therefore, the impedance of fractal EBG is more capacitive than conventional EBG. The real and imaginary parts of the impedance of conventional and fractal EBGs are shown in Fig. 6. The band notch frequency decreases due to an increase in capacitance in fractal EBG as shown in Fig. 7.

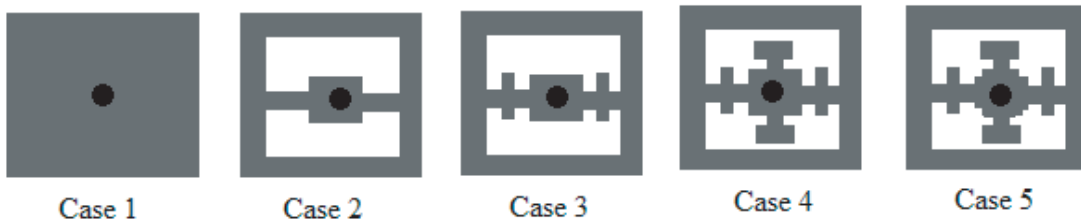


Figure 5. Evolution of fractal EBG structures.

2.4. Two Edge Located Via (TVEL) EBG

The proposed TVEL and conventional TVEL EBG are shown in Fig. 8. The unit element of two EBGs have the same size of $6 \times 6 \text{ mm}^2$. The TVEL EBG in proposed antenna rejects WiMAX and X band (3.4–4.4) GHz and (7.2–7.7) GHz, respectively. To design a compact EBG structure, the effective values for C and L are increased. Evolution of the proposed TVEL EBG structure is shown in Fig. 9. Metallic strips are introduced to increase the metallic surface area and decrease the inductance. The decrease

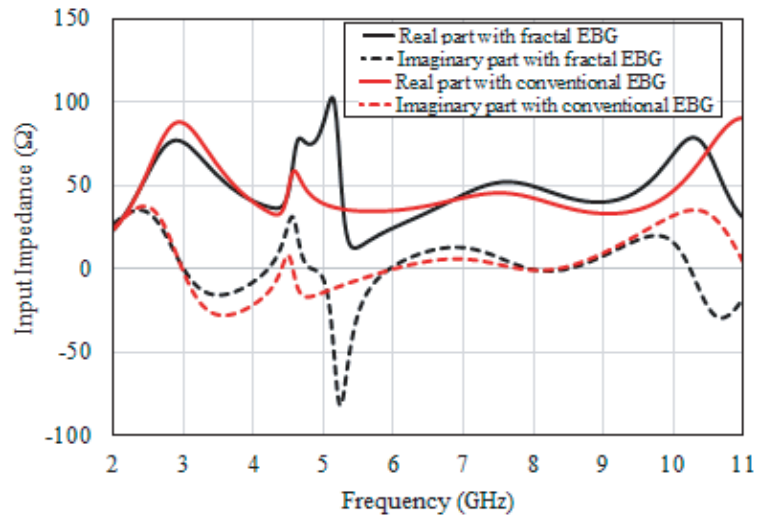


Figure 6. Real and imaginary impedances with Fractal and conventional EBG.

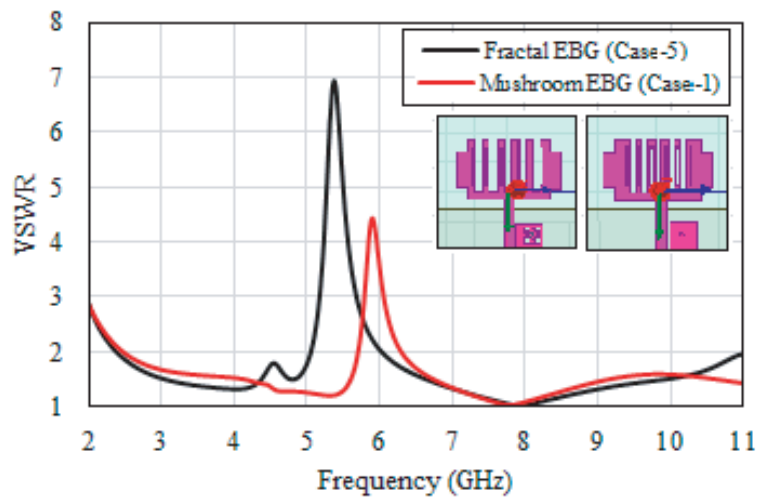


Figure 7. VSWR plot of fractal and conventional EBGs.

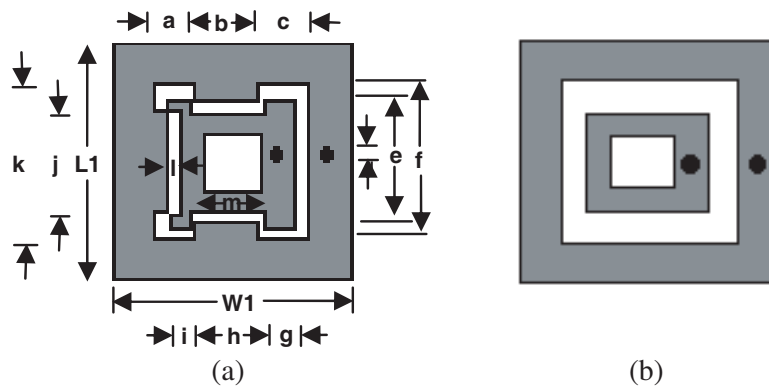


Figure 8. Geometries of the EBGs. (a) Proposed TVEL EBG. (b) Conventional TVEL EBG.

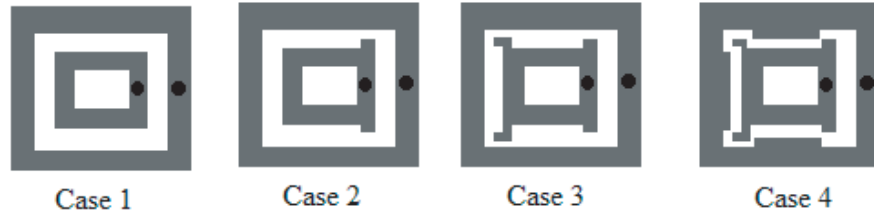


Figure 9. Evolution of the proposed TVEL EBG structures.

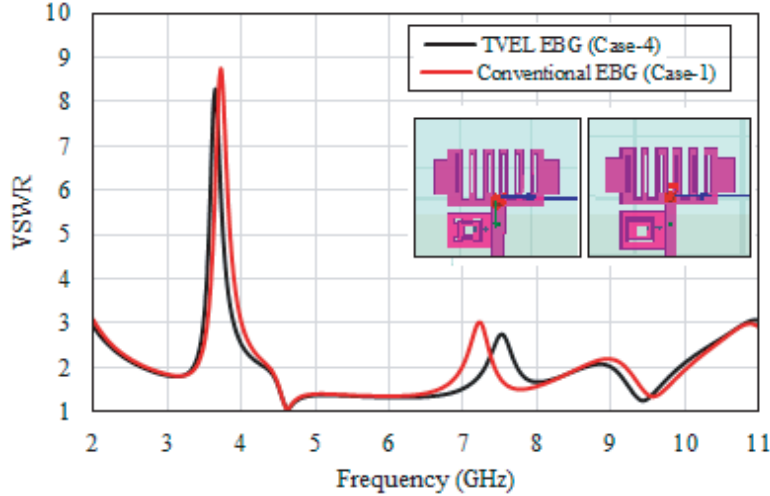


Figure 10. VSWR plot of proposed TVEL and Conventional EBG.

in the gap between the slots increases the capacitance. Outer metallic ring and the gap between the two metallic rings determine the lower band notch frequency. As the surface area increases, inductance decreases, but the capacitance increases due to decrease in gap between the slots. As a result, there is a small decrease in central frequency of the lower band notch. The dimensions of the inner metallic ring determine the upper band notch frequency. Since slot dimensions of the inner ring remain same, capacitance remains same, whereas the inductance decreases due to an increase in metallic surface area; therefore, the central frequency of the upper band notch increases. Hence, by optimizing the parameters of TVEL EBG structure, both lower and upper band notches can be controlled. VSWR plots of the proposed TVEL and conventional EBG are shown in Fig. 10.

The parameters for TVEL-EBG are: $W1 = 6$ mm, $L1 = 6$ mm, $a = 1$ mm, $b = 1.6$ mm, $c = 1.3$ mm, $e = 3.2$ mm, $f = 3.9$ mm, $g = 0.88$ mm, $h = 1.84$ mm, $i = 0.55$ mm, $j = 2.5$ mm, $k = 3.9$ mm, $m = 1.38$ mm, $l = 0.324$ mm, $d = 0.78$ mm.

2.5. Effect of Position of EBG Structures

EBG structures are capacitively coupled to feed line. At the central band notch frequency, EBG structures get strongly coupled to feed line, and the antenna becomes non-responsive at these band notch. As the gap between the EBG structure is increased, the capacitive coupling decreases, and the central band notch frequency of the middle band increases due to decrease in capacitance between the feed line and fractal EBG. Also, band notch characteristics degrade, and the maximum VSWR value of the band notch decreases with increase in the gap between the feed line and fractal EBG as shown in Fig. 11.

There is a little effect on the lower band notch due to a small variation in the gap between the feed line and TVEL EBG. However, as the gap increases, the capacitance between the gap and feed line decreases. The inductance also decreases due to decrease in surface current on the outer metallic strip.

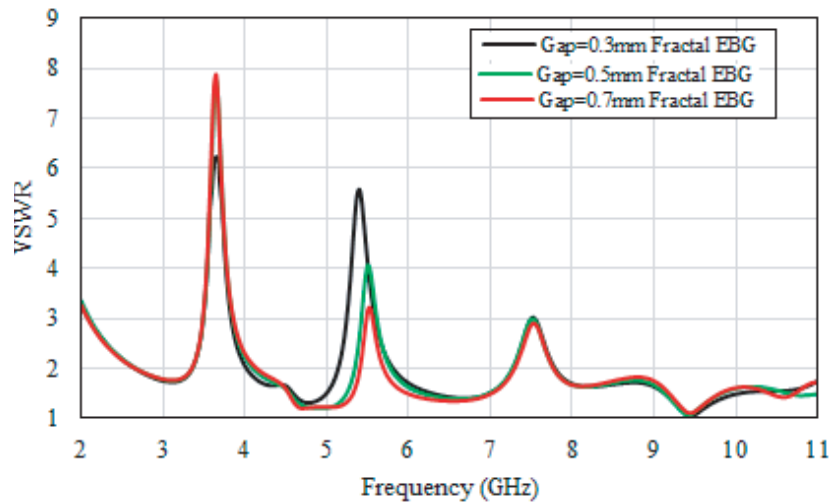


Figure 11. VSWR of gap between fed line and Fractal EBG structure.

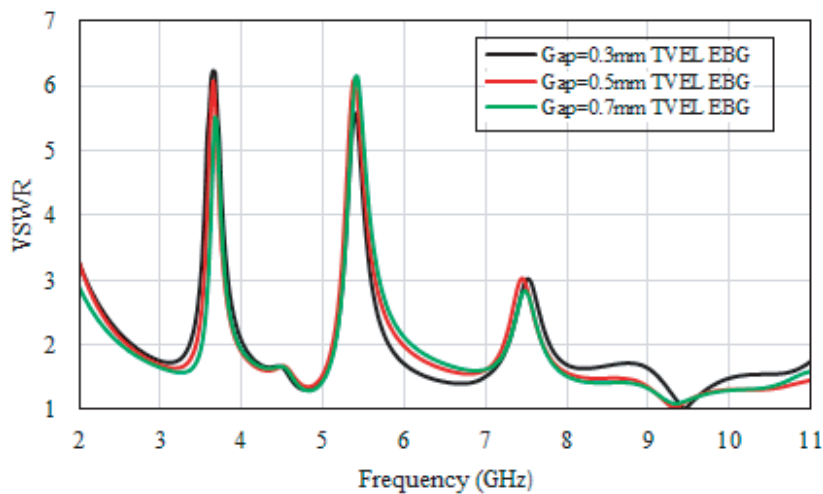


Figure 12. VSWR of gap between fed line and TVEL EBG structure.

As a result, the central band notch frequency of the lower band increases marginally with increase in the gap. The surface current on the inner ring and inductance decreases with increase in gap. As a result, the central frequency of upper band notch increases with increase in gap between the feed line and TVEL EBG as shown in Fig. 12. Combined effect of gap between the fractal and TVEL EBG structures and feed line on the three band notch frequencies is shown in Fig. 13. Since the EBG structures are placed near the feed line, the proposed EBG structures can be incorporated in other UWB antennas to achieve the desired band notches.

To validate the bandgap characteristics of EBG cell, it is simulated in eigenmode solution, and dispersion diagram based on rectangular (irreducible) Brillouin zone is plotted as depicted in Fig. 14. Two band gaps exist in TVEL-EBG, and one band gap exists in fractal EBG structure as shown in Figs. 10(a) and 4(b), respectively. The first band gap (grey part) is between mode 1 and mode 2, centered at $f_{c1} = 3.45$ GHz with lower cutoff frequency $f_{l1} = 3.1$ GHz and higher cutoff frequency $f_{h1} = 3.8$ GHz. The second band gap (red part) is present between mode 2 and mode 3 centered at $f_{c3} = 7.25$ GHz, with lower and higher cutoff frequencies of $f_{l3} = 7.0$ GHz and $f_{h3} = 7.5$ GHz, respectively. For fractal EBG first band gap (green part) is between mode 1 and mode 2 centered at $f_{c2} = 5.15$ GHz with lower and higher cutoff frequencies of $f_{l2} = 4.8$ GHz and $f_{h2} = 5.5$ GHz, respectively.

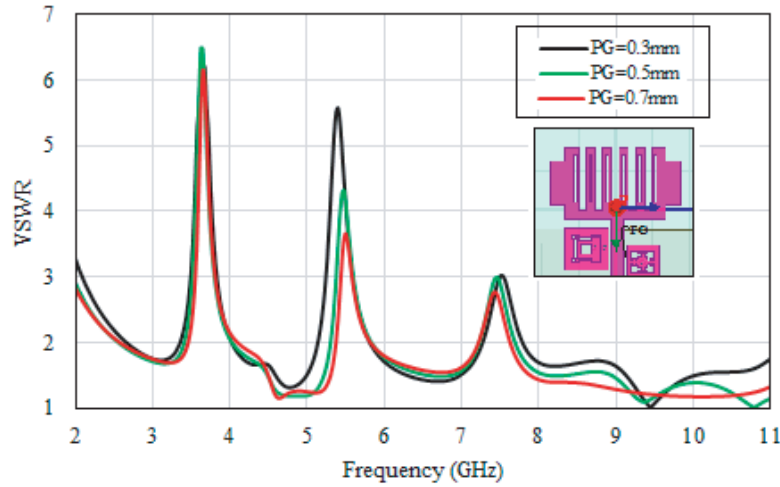


Figure 13. VSWR of gap between fed line and two EBGs structure.

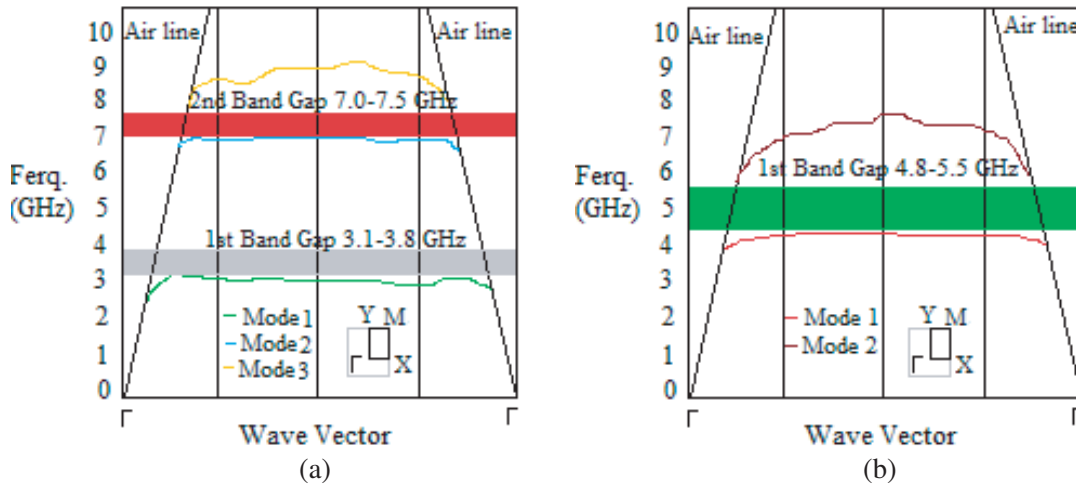


Figure 14. Dispersion diagram for (a) TVEL EBG structure, (b) Fractal EBG.

3. SIMULATION AND MEASUREMENT RESULTS

The proposed antenna is fabricated on an FR4 substrate and tested using an Agilent VNA (8722ET). The prototype antenna, and simulated and measured VSWRs are shown in Fig. 15 and Fig. 16, respectively. Structure with EBG has triple band notches at 3.65 GHz (3.3–4.0 GHz), 5.45 GHz (5.1–5.8 GHz) and 7.5 GHz (7.2–7.8 GHz), thus TVEL-EBG offers dual-band gap, and fractal EBG provides single band gap characteristics. Measured results agree with simulated ones.

Figure 17 shows the surface current distribution at three centre notched frequencies at 3.65 GHz, 5.45 GHz, and 7.5 GHz, respectively. When the antenna operates at the first notch 3.65 GHz and third notch 7.5 GHz, high concentration of surface current in the TVEL-EBG structure indicates the band notch, while the concentration of surface current distribution at 5.45 GHz indicates the second notch. The real and imaginary impedance variations of the proposed antenna with and without EBG are presented in Fig. 18. Real part of the impedance due to EBG structures tends to be $+\infty$ (positively high) while the imaginary part tends towards $-\infty$ (negatively high) resulting in band notch characteristics.

The gain and efficiency of the proposed antenna are shown in Fig. 19(a) and Fig. 19(b). The maximum gain is 5.1 dBi at 8 GHz. Gain varies from 1.8 dBi to 5.1 dBi over the UWB except at notched

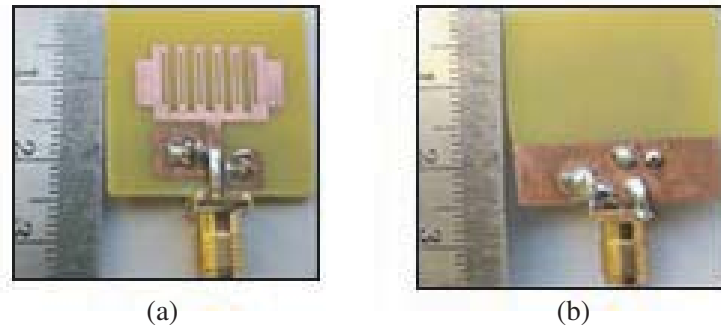


Figure 15. Photographs of the fabricated antenna: (a) top view; (b) bottom view.

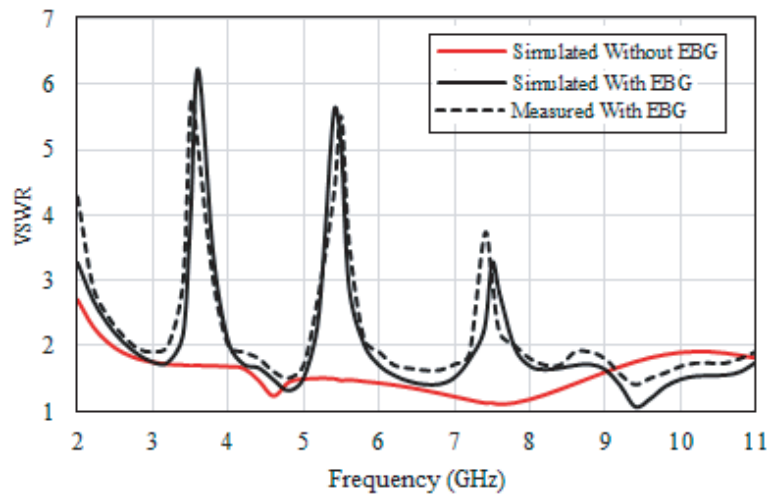


Figure 16. Simulated and measured VSWR of UWB antenna without EBG and with TVEL EBG and fractal EBG.

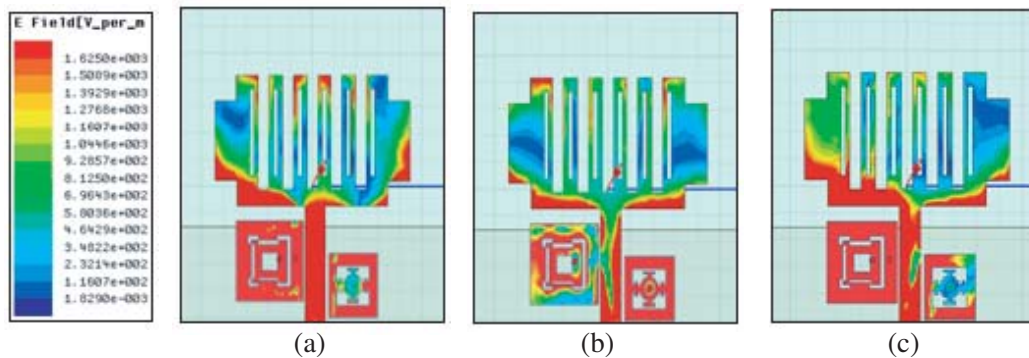


Figure 17. Surface current distribution at the frequency of (a) 3.65 GHz (b) 5.45 GHz. (c) 7.5 GHz.

bands. The averaged efficiency of the proposed antenna is 82% with a peak efficiency of 89%.

Radiation patterns in the E-plane and H-plane at 3.00 GHz, 5.00 GHz, and 9.00 GHz are shown in Fig. 20. There is a little tilt in radiation patterns at 9.00 GHz frequency. The antenna offers nearly omnidirectional patterns in H-plane and nearly figure of 8 patterns in E-plane.

Comparison of the proposed antenna with reported state of art antennas using EBG structures is listed in Table 1. The proposed antenna is smaller in size and uses only 2 EBG structures viz. TVEL and fractal EBG as compared to all reported antennas.

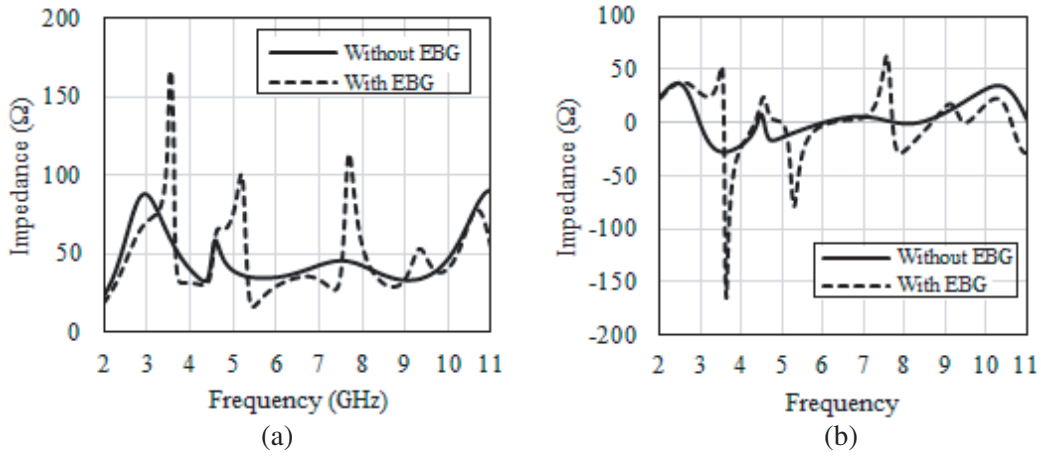


Figure 18. Impedances of UWB antenna without EBG and with EBG (a) real part, and (b) imaginary part.

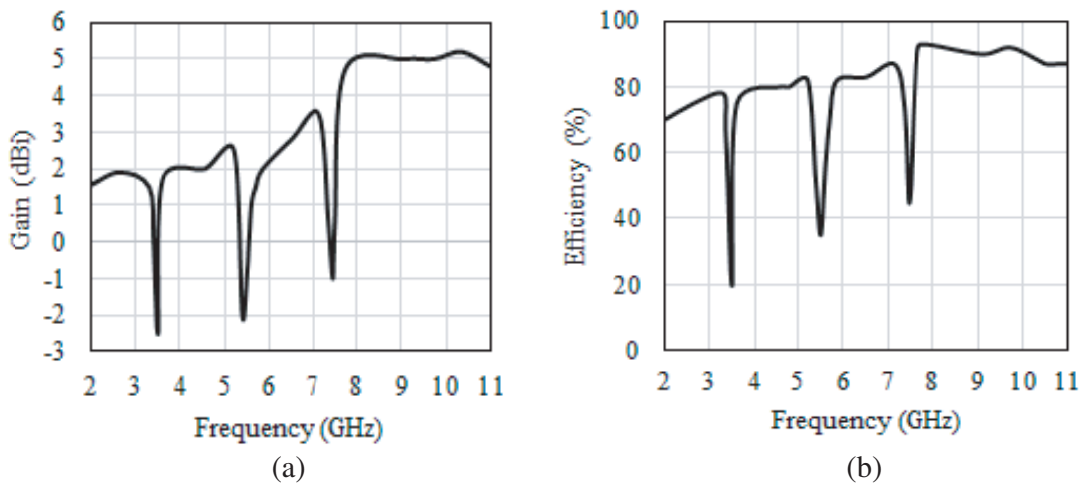
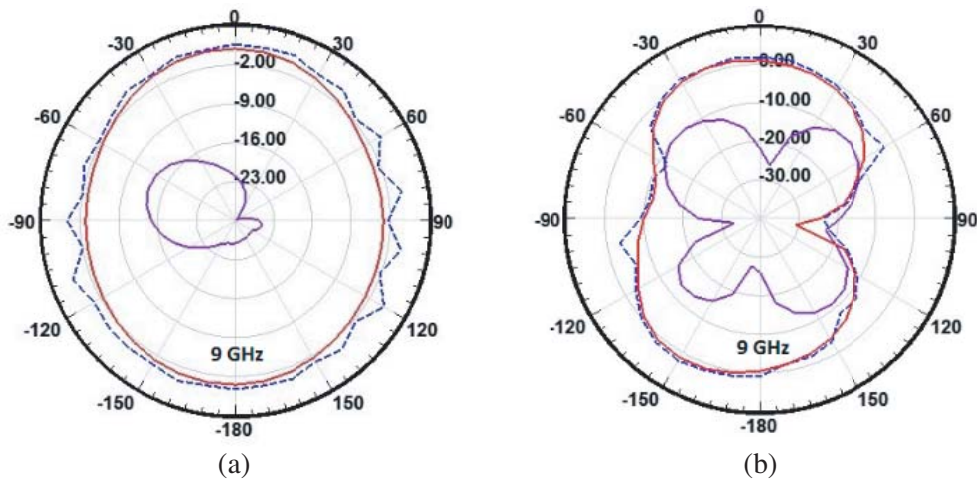


Figure 19. (a) Gain of proposed antenna. (b) Efficiency of proposed antenna.



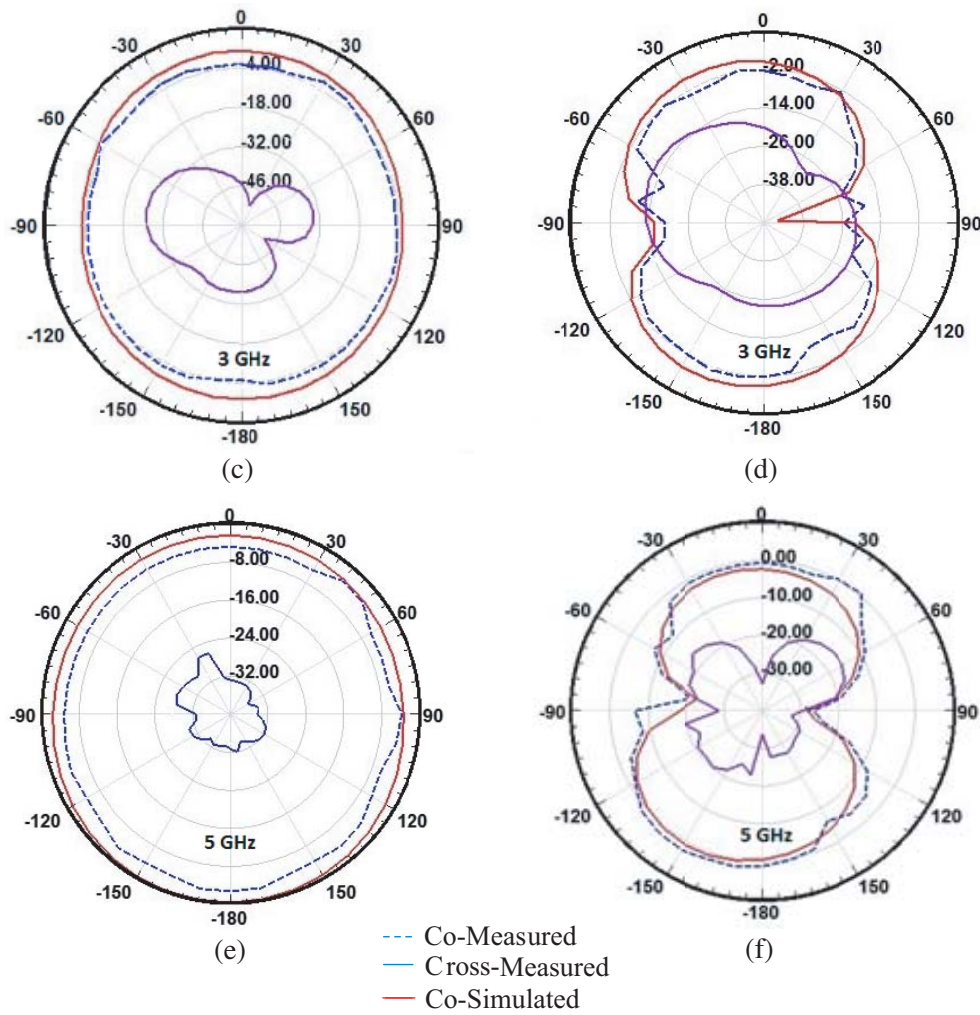


Figure 20. Comparison of measured and simulated radiation patterns of the proposed antenna: (a), (c), and (e) *H*-plane, (b), (d), and (f) *E*-plane.

Table 1. Comparison of TVEL-EBG and Fractal EBG structures to other EBG structures used for Band notch in UWB antenna.

Ref.	Size (mm ²)	Type of EBG	ϵ_r/h	No. of EBG	No. of Band notched
12	39 × 35	CMT	3.38/0.8	04	Single
13	38 × 40	ELV	4.5/1	01	Single
14	30 × 35	Spiral	3.66/0.762	02	Dual
15	42 × 50	CMT	4.4/1.6	04	Dual
16	42 × 50	CMT	4.4/1.6	02	Dual
17	38 × 40	TVDS	4.4/0.8	01	Dual
Proposed	24 × 24	TVEL/Fractal	4.4/1.6	02	Triple

4. CONCLUSION

In this paper, a novel compact UWB antenna is designed with triple band-notched characteristics using TVEL-EBG and fractal EBG structure. $VSWR \leq 2$ is obtained over UWB from 2.9 GHz to 11.2 GHz with band notches at WiMAX (3.3–4.0 GHz), WLAN (5.1–5.8 GHz), and satellite downlink communication (7.2–7.8 GHz). The proposed technique using EBG structures near the feed line can be incorporated in other UWB antennas also to achieve the desired band notches. The proposed antenna offers high efficiency and nearly omnidirectional radiation pattern.

REFERENCES

1. First Report and order, "Revision of part 15 of the commission's rule regarding ultra-wideband transmission system FCC 02-48," Federal Communication Commission, 2001.
2. Ibrahim, A. A., M. A. Abdalla, and A. Boutejdar, "Printed compact band-notched antenna using octagonal radiating patch and meander slot technique for UWB applications," *Progress In Electromagnetics Research M*, Vol. 54, 153–162, 2017.
3. Srivastava, K., A. Kumar, B. K. Kanaujia, S. Dwari, A. K. Verma, K. P. Esselle, and R. Mittra, "Integrated GSM-UWB Fibonacci-type antennas with single, dual, and triple notched bands," *IET Microwaves, Antennas & Propagation*, Vol. 12, No. 6, 1004–1012, 2018.
4. Singh, A. P., R. Khanna, and H. Singh, "UWB antenna with dual notched band for WiMAX and WLAN application," *Microwave and Optical Technology Letters*, Vol. 59, No. 4, 792–797, 2017.
5. Hammache, B., A. Messai, I. Messaoudene, and T. A. Denidni, "A compact ultra-wideband antenna with three C-shaped slots for notched band characteristics," *Microwave and Optical Technology Letters*, Vol. 61, 275–279, 2018.
6. Yadav, A., M. D. Sharma, and R. P. Yadav, "A CPW-fed CSRR and inverted U slot loaded triple band notched UWB antenna," *Progress In Electromagnetics Research C*, Vol. 89, 221–231, 2019.
7. Rehman, S. U. and M. A. S. Alkanhal, "Design and system characterization of ultra-wideband antennas with multiple band-rejection," *IEEE Access*, Vol. 5, 17988–17996, 2017.
8. Shaik, L. A., C. Saha, J. Y. Siddiqui, and Y. M. M. Antar, "Ultra-wideband monopole antenna for multiband and wideband frequency notch and narrowband applications," *IET Microwaves, Antennas & Propagation*, Vol. 10, No. 11, 1204–1211, 2016.
9. Mansouri, Z., A. S. Arezomand, S. Heydari, and F. B. Zarrabi, "Dual notch UWB fork monopole antenna with CRLH metamaterial load," *Progress In Electromagnetics Research C*, Vol. 65, 111–119, 2016.
10. Vendik, I. B., A. Rusakov, K. Kanjanasit, J. Hong, and D. Filonov, "Ultra-Wideband (UWB) planar antenna with single, dual and triple-band notched characteristic based on electric ring resonator," *IEEE Antennas and Wireless Propagation Letters*, Vol. 16, 1597–1600, 2017.
11. Liu, B.-W., Y.-Z. Yin, Y. Yang, S.-H. Jing, and A.-F. Sun, "Compact UWB bandpass filter with two notched bands based on electromagnetic bandgap structures," *Electronics Letters*, Vol. 47, No. 13, 757–758, 2011.
12. Yazdi, M. and N. Komjani, "Design of a band-notched UWB monopole antenna by means of an EBG structure," *IEEE Antennas and Wireless Propagation Letters*, Vol. 10, 170–173, 2011.
13. Peng, L. and C.-L. Ruan, "UWB band-notched monopole antenna design using electromagnetic-bandgap structures," *IEEE Transactions on Microwave Theory and Techniques*, Vol. 59, No. 4, 1074–1081, 2011.
14. Xu, F., Z. X. Wang, X. Chen, and X.-A. Wang, "Dual band-notched UWB antenna based on spiral electromagnetic-bandgap structure," *Progress In Electromagnetics Research B*, Vol. 39, 393–409, 2012.
15. Jaglan, N., B. K. Kanaujia, S. D. Gupta, and S. Srivastava, "Design and development of an efficient EBG structures based band notched UWB circular monopole antenna," *Wireless Personal Communications*, Vol. 96, No. 4, 5757–5783, 2017.

16. Jaglan, N., S. D. Gupta, B. K. Kanaujia, and S. Srivastava, "Band notched UWB circular monopole antenna with inductance enhanced modified mushroom EBG structures," *Wireless Personal Communications*, Vol. 24, No. 2, 383–393, 2018.
17. Bhavarthe, P., S. Rathod, and K. T. V. Reddy, "A compact dual band electromagnetic band gap structure," *IEEE Transactions on Antennas and Propagation*, Vol. 67, No. 1, 596–600, 2019.
18. Yang, F. and Y. Rahmat-Samii, "Microstrip antennas integrated with Electromagnetic Band-Gap (EBG) structures: A low mutual coupling design for array applications," *IEEE Transactions on Antennas and Propagation*, Vol. 51, No. 10, 2936–2946, 2003.